Numerical Rock Physics: Fluid effects on wave propagation

E.H. Saenger, O.S. Krüger, and S.A. Shapiro

email: *saenger@geophysik.fu-berlin.de*

keywords: *Gassmann equation, Biot's velocity relations, dry and fluid-saturated rocks, rotated staggered grid, finite differences, numerical rock physics*

ABSTRACT

This paper is concerned with numerical considerations of fluid effects on wave propagation. The focus is on effective elastic properties (i.e. velocities) in different kinds of dry and fluid-saturated fractured media. We apply the so-called rotated staggered finite-difference grid (RSG) technique. Using this modified grid it is possible to simulate the propagation of elastic waves in a 2D or 3D medium containing cracks, pores or free surfaces without explicit boundary conditions and without averaging elastic moduli. Therefore the RSG allows an efficient and precise numerical study of effective velocities in fractured structures. We simulate the propagation of plane waves through three kinds of randomly cracked 3D media. Each model realization differs in the porosity of the medium and is performed for dry and fluid-saturated pores. The synthetic results are compared with the predictions of the well known Gassmann equation and the Biot velocity relations. Although we have a very low porosity in our models, the numerical calculations showed that the Gassmann equation cannot be applied for isolated pores (thin penny-shaped cracks). For Fontainebleau sandstone we observe with our dynamic finite-difference approach the exact same elastic properties as with a static finite-element approach. For this case the Gassmann equation can be checked successfully. Additionally, we show that so-called open-cell Gaussian random field models are an useful tool to study wave propagation in fluid-saturated fractured media. For all synthetic models considered in this study the high-frequency limit of the Biot velocity relations is very close to the predictions of the Gassmann equation.

INTRODUCTION

The problem of effective elastic properties of fractured solids is of considerable interest for geophysics, material science, and solid mechanics. Strong scattering caused by complex rock structures can be treated only by numerical techniques since an analytical solution of the wave equation is not available. In this paper we consider the problem of a fractured medium in three dimensions. Alternative numerical studies of elastic moduli of porous media of Arns et al. (2002) and Roberts and Garboczi (2002) employ a (static) finite-element method (FEM). This FEM uses a variational formulation of the linear elastic equations and finds the solution by minimising the elastic energy using a fast conjugate-gradient model. Dynamic attenuation effects can not be described with this method. Finite difference (FD) methods discretise the wave equation on a grid. They replace spatial derivatives by FD operators using neighbouring points. This discretisation can cause instability problems on a staggered grid when the medium contains high contrast discontinuities (strong heterogeneities). These difficulties can be avoided by using the rotated staggered grid (RSG) technique (Saenger et al., 2000; Saenger and Bohlen, 2004). Since the FD approach is based on the wave equation without physical approximations, the method accounts not only for direct waves, primary reflected waves, and multiply reflected waves, but also for surface waves, head waves, converted reflected waves, and waves observed in ray-theoretical shadow zones (Kelly et al. 1976). The main objective of this paper is a numerical study of effective elastic properties of fractured 3D-media with connected pores [numerical results of fractured 2D- and 3D- media with isolated cracks can be found in Saenger and

Shapiro (2002), Saenger et al. (2002) and Orlowsky et al. (2004)]. Here we simulate the propagation of plane waves through a well defined fractured region with dry or fluid-filled pores.

THE GASSMANN EQUATION

The Gassmann equation (Gassmann 1951) predicts the elastic moduli of a fluid-saturated porous media using the known elastic moduli of the solid matrix, the frame and the pore fluid:

$$\frac{K_{\text{sat}}}{K_0 - K_{\text{sat}}} = \frac{K_{\text{dry}}}{K_0 - K_{\text{dry}}} + \frac{K_{\text{fl}}}{\phi(K_0 - K_{\text{fl}})} \quad (1)$$

$$\mu_{\text{sat}} = \mu_{\text{dry}} \quad (2)$$

$$\rho_{\text{sat}} = \rho_{\text{dry}} + \phi\rho_{\text{fl}} \quad (3)$$

where:

K_{dry}	effective bulk modulus of dry rock frame
K_{sat}	effective bulk modulus of the rock with pore fluid
K_0	bulk modulus of mineral making up rock
K_{fl}	effective bulk modulus of pore fluid
ϕ	porosity
μ_{dry}	effective shear modulus of dry rock
μ_{sat}	effective shear modulus of rock with pore fluid
ρ_{sat}	density of the rock with pore fluid
ρ_{dry}	density of the dry rock frame
ρ_{fl}	pore fluid density

BASIC ASSUMPTIONS IN THE GASSMANN EQUATION

The basic assumptions in the Gassmann equation are Wang and Nur (2000):

1. the rock or porous medium (both the matrix and the frame) is macroscopically homogeneous and isotropic;
2. all the pores are interconnected or communicating;
3. the pores are filled with a frictionless fluid (liquid, gas or mixture);
4. the rock-fluid system under study is closed (undrained);
5. the relative motion between the fluid and the solid is negligibly small compared to the motion of the saturated rock itself when the rock is excited by a wave; and
6. the pore fluid does not interact with the solid in a way that would soften or harden the frame.

THE SYNTHETIC FRACTURE-MODELS

In order to consider fluid effects on wave propagation we design a number of synthetic fracture-models (size: 400^3 gridpoints) with a well known number of pores or porosity. We consider three different types of fractured media:

- **Type 1:** The fractured region is filled at random with randomly oriented non-intersecting thin **penny-shaped cracks**. A typical model is shown in Figure 1. In the Gassmann equation both phases, the fluid and the mineral, are assumed to be continuous. This is not the case for isolated cracks. However, we want to numerically clarify if the Gassmann-equation can be used for such configurations in the low-porosity limit.

Figure 1: Non-intersecting thin penny-shaped cracks

- **Type 2:** The second model (Figure 2) is a microtomographic image of **Fontainebleau sandstone**. We use a 400^3 cubic set of the model fb7.5 of Arns et al. (2002). Therefore, our numerical estimates of effective elastic properties derived with our dynamic FD approach can be directly compared with the results of the static approach of Arns et al. (2002).

- **Type 3:** To generate realistic synthetic microstructures we use the approach described in Roberts and Garboczi (2002), the so-called **open-cell Gaussian random field (GRF)** scheme. To ensure a 100% connectivity of the pores we eliminate isolated pores. Some details of our models used are listed in Table 1. Figure 3 shows two different realizations. The similarity to the microtomographic image of Fontainebleau sandstone (Figure 2) for the model with the lower porosity is amazing.

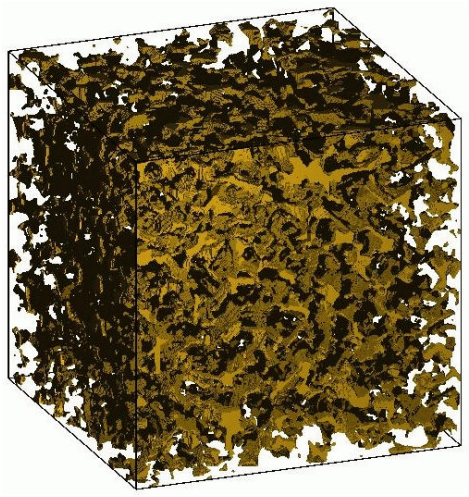

Figure 2: A X-ray microtomographic image of Fontainebleau sandstone (porosity $\phi = 0.084$). The structure shown is the porespace, the transparent part is the rock frame. For details refer to Arns et al. (2002).

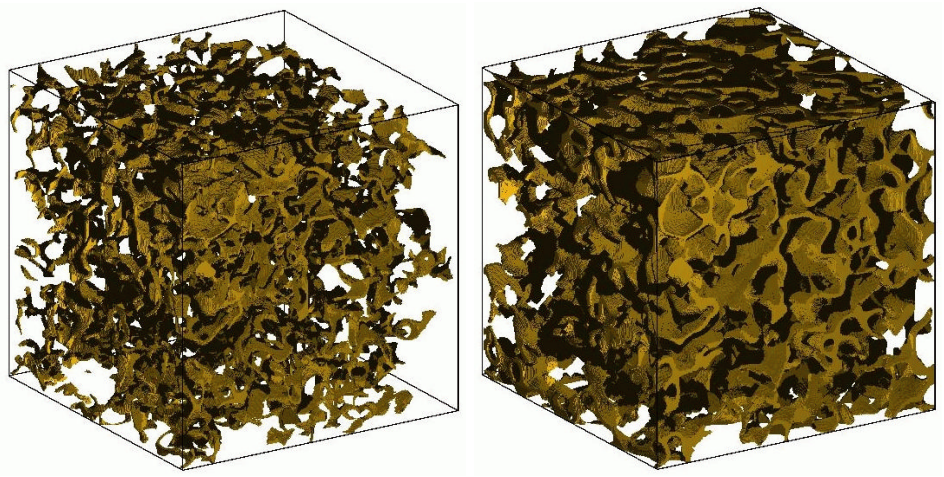

Figure 3: Two open-cell Gaussian random fields (GRF). Top: porosity $\phi = 0.034$. Bottom: porosity $\phi = 0.1322$. For details refer to Roberts and Garboczi (2002).

MEDIUM:	GRF 1 ($\phi = 0.0342$)	GRF 2 ($\phi = 0.0877$)	GRF 3 ($\phi = 0.1322$)	GRF 4 ($\phi = 0.0802$)
Gaussian 1				
corr. len. [0.0002m]	25	25	25	13
$0 <$ cut min. < 1	0.4	0.4	0.4	0.4
$0 <$ cut max. < 1	0.6	0.6	0.6	0.6
Gaussian 2				
corr. len. [0.0002m]	30	30	30	15
$0 <$ cut min. < 1	0.485	0.48	0.4575	0.4904
$0 <$ cut max. < 1	0.515	0.52	0.5415	0.5296

Tab. 1: Some details concerning the GRF-models used in our numerical study.

MODELING PROCEDURE

The synthetic fracture-models are embedded in a homogeneous region. The full models are made up of 804 $\times$ 400 $\times$ 400 grid points with an interval of 0.0002m. In the homogeneous region we set $v_p = 5100\ m/s$, $v_s = 2944\ m/s$ and $\rho_g = 2540\ kg/m^3$. For the dry pores we set $v_p = 0\ m/s$, $v_s = 0\ m/s$ and $\rho_g = 0.0001\ kg/m^3$ which approximates vacuum. For the fluid-filled pores we set $v_p = 1500\ m/s$, $v_s = 0\ m/s$ and $\rho_g = 1000\ kg/m^3$ which approximates water. It is important to note that we perform our Modeling experiments with periodic boundary conditions in the two horizontal directions. For this reason our synthetic penny-shaped crack and GRF models are generated also with this periodicity. To obtain effective velocities in different models we apply a body force plane source at the top of the model. The plane wave generated in this way propagates through the fractured medium (see Figure 5). With two horizontal planes of geophones at the top and at the bottom, it is possible to measure the time-delay of the mean peak amplitude of the plane wave caused by the inhomogeneous region. With the time-delay one can estimate the effective velocity. Additionally, the attenuation of the plane wave can be studied. The source wavelet in our experiments is always the first derivative of a Gaussian with a dominant frequency of $8 * 10^5\ 1/s$ and with a time increment of $\Delta t = 2.1 * 10^{-9} s$. The resulting power spectrum of the plane wave is shown in Figure 4. From the modelling point of view it is important to note that all computations are performed with second order spatial FD operators and with a second order time update. Due to the size of the models we have to use large-scale computers (e.g. CRAY T3E) with a MPI implementation of our modelling software.

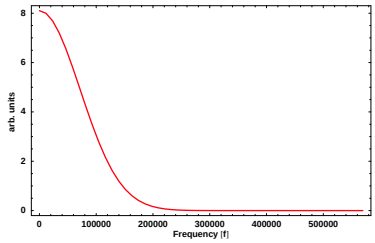

Figure 4: Power-spectrum of the generated plane wave.

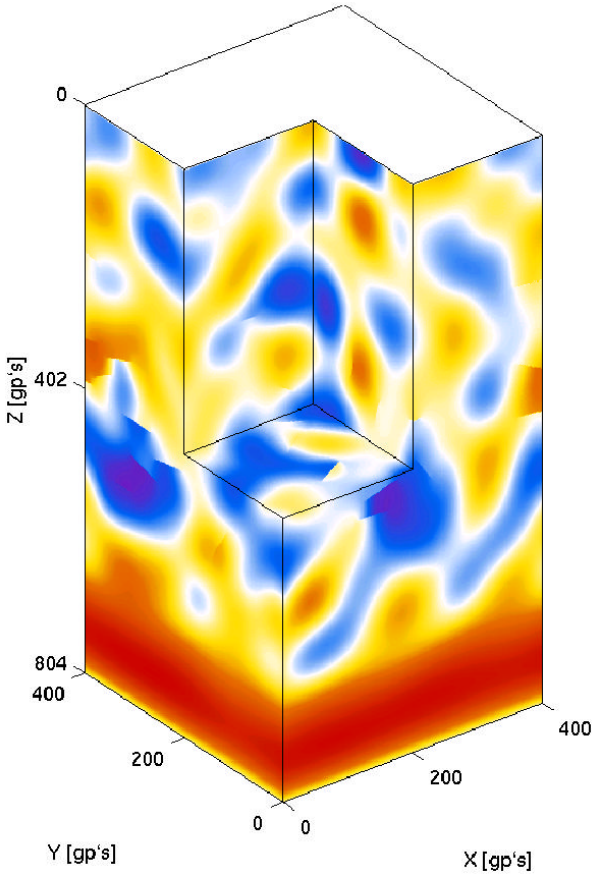

Figure 5: A displacement-snapshot of a plane wave propagating through a fractured 3D model with penny shaped cracks. We use a non-linear colorscale to emphasise the scattered wavefield.

NUMERICAL RESULTS

Our numerical setup enables us to compare 3D fractured media with exact the same pore positions for fluid-filled and for empty pores (i.e. the dry rock frame is exactly the same in both simulations). Therefore we can test the applicability of the Gassmann-equation and the Biot velocity relations [see e.g. Mavko et al. (1998)] for our 3D fractured materials without any additional effective medium theory. For all synthetic models we fulfil the assumptions (1), (3), (4) and (6) of the Gassmann equation (discussed above).

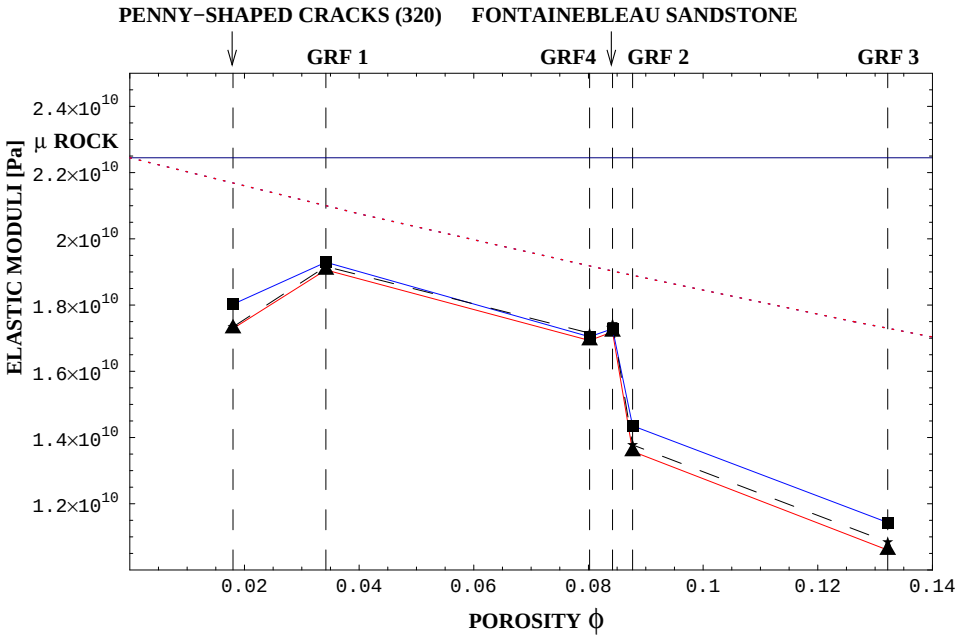

Figure 6: Effective shear (μ) moduli versus porosity for six different synthetic fracture models. μ DRY [triangles joined with a (red) solid line] and μ SAT [boxes joined with a (blue) solid line] are estimated from numerical velocity measurements using the rotated staggered finite-difference grid (for each synthetic fracture model we have exact the same rock frame). The high-frequency limit of the Biot velocity relations [stars joined with a (black) dashed line] is calculated using μ DRY. The shear modulus of the rock frame is displayed with a horizontal line; the dotted line displays the upper Hashin-Shtrikman bound.

Penny-shaped cracks

The calculated normalised effective moduli for fluid-filled and for empty non-intersecting cracks (model type 1) are compared in Figure 6 and 7. There is a relative big difference between the shear moduli of the models below the range of the connectivity percolation threshold. This bring us to the conclusion that the Gassmann-equation cannot be applied to isolated fluid-filled cracks even with a low porosity in the used models. From a practical point of view this has the following well-known consequence: If one applies the Gassmann-equation one has to distinguish between the isolated fraction and the continuous fraction of the fluid. The isolated fluid fraction should be considered as a part of the 'dry' rock frame.

Fontainebleau Sandstone

The calculated normalised effective shear moduli μ^*/μ_0 for the dry and fluid-saturated Fontainebleau sandstone (model type 2) are 0.766 and 0.770, respectively (compare with Figure 6. For this model the prediction of the Gassmann equation (equation 2) is very accurate. Moreover, our dynamic approach gives approximately the same result as the static approach of Arns et al. (2002) [$\mu^*/\mu_0 \approx 0.765$, for the dry and fluid-saturated case from Figure 5b of Arns et al. (2002)]. This is very interesting because the connectivity of the pores is not 100% perfect (compare with assumption (2) of the Gassmann equation). The numerical estimated bulk modulus (Figure 7) is also in good agreement with the theoretical predictions of the Gassmann equation and the high frequency limit of the Biot velocity relations.

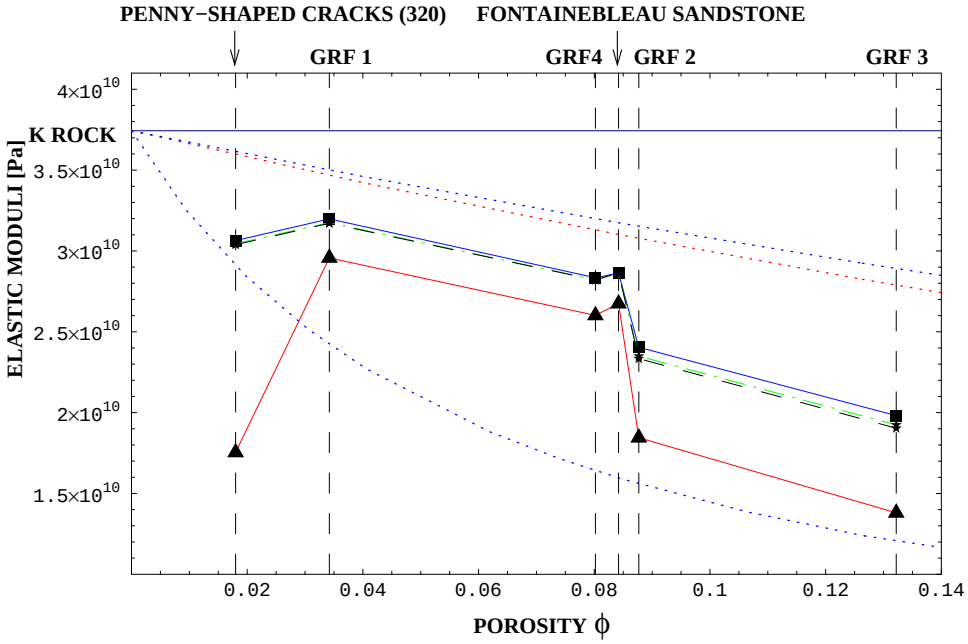

Figure 7: Effective bulk (K) moduli versus porosity for six different synthetic fracture models. K DRY [triangles joined with a (red) solid line] and K SAT [boxes joined with a (blue) solid line] are estimated from numerical velocity measurements using the rotated staggered finite-difference grid (for each synthetic fracture model we have exact the same rock frame). K GAS [stars joined with a (green) dashed-dotted line] is calculated using the Gassmann-equation with μ DRY and K DRY. The high-frequency limit of the Biot velocity relations [stars joined with a (black) dashed line] is also calculated using μ DRY and K DRY. The bulk modulus of the rock frame is displayed with a horizontal line; the dotted lines display the Hashin-Shtrikman bounds.

Open-cell Gaussian random fields (GRF)

The calculated normalised effective moduli for the open-cell Gaussian random field models are shown in Figure 6 and 7. With an increase of the porosity (GRF 1, GRF 2 and GRF 3) we observe an increasing mismatch between the predictions of the Gassmann equation (equation 2) and our numerical results. As mentioned above, the connectivity of pores for the open-cell GRF models [assumption (2)] is 100%. Therefore, we explain this mismatch with the relative large structures of the open-cell GRF models compared to the Fontainebleau sandstone model. Note, the Gassmann equation is only valid in the long wavelength limit [connected with assumption (5)]. However, the mismatch for a porosity of $\phi = 0.034$ is about 1%. This is a promising starting point for our numerical considerations to fulfil all assumptions [from (1) to (6)] of the Gassmann equation. A first step in this direction is the model GRF 4 with the appendant numerical results of elastic moduli shown in Figure 6 and 7.

CONCLUSIONS

Finite-difference modelling of the elastodynamic wave equation is very fast and accurate. We use the rotated staggered FD grid to calculate elastic wave propagation in fractured media. Our numerical modelling of elastic properties of dry rock skeletons can be considered as an efficient and well controlled computer experiment. In this paper we consider 3D isotropic dry and fluid-saturated fractured media. We have tested the applicability of numerical methods to these media with respect to the predictions of the Gassmann equation and the Biot velocity relations. As for measured data [laboratory experiments, see Wang (2002)] our synthetic data usually gives higher effective properties for the fluid-saturated rocks as predicted by

the Gassmann equation. For isolated thin penny-shaped cracks the standard Gassmann equation cannot be applied although we have a very low porosity in our models. For the Fontainebleau sandstone model we obtain with our dynamic FD approach exactly the same elastic properties as the static approach applied in Arns et al. (2002). For this model the Gassmann equation can be verified. Additionally, we show that so-called open-cell Gaussian random field models are a useful synthetic database to consider fluid-saturated 3D fractured media.

ACKNOWLEDGEMENTS

This work was kindly supported by the sponsors of the *Wave Inversion Technology (WIT) Consortium*, Berlin, Germany.

REFERENCES

Arns, C. H., Knackstedt, M. A., Pinczewski, W. V., and Garboczi, E. J. (2002). Computation of linear elastic properties from microtomographic images: Methodology and agreement between theory and experiment. *Geophysics*, 67:1396–1405.

Gassmann, F. (1951). Über die Elastizität poröser Medien. *Vier. der Natur Gesellschaft*, 96:1–23.

Kelly, K. R., Ward, R. W., Treitel, S., and Alford, R. M. (1976). Synthetic seismograms: A finite-difference approach. *Geophysics*, 41:2–27.

Mavko, G., Mukerji, T., and Dvorkin, J. (1998). *The Rock Physics Handbook*. Cambridge University Press, Cambridge.

Orlowsky, B., Saenger, E. H., Guéguen, Y., and Shapiro, S. A. (2004). Effects of parallel crack distributions on effective elastic properties - a numerical study. *International Journal of Fractures*, page in print.

Roberts, A. P. and Garboczi, E. J. (2002). Computation of the linear elastic properties of random porous materials with a wide variety of microstructure. *Proc. R. Soc. Lond. A*, 458:1033–1054.

Saenger, E. H. and Bohlen, T. (2004). Anisotropic and viscoelastic finite-difference modeling using the rotated staggered grid. *Geophysics*, 69:in print.

Saenger, E. H., Gold, N., and Shapiro, S. A. (2000). Modeling the propagation of elastic waves using a modified finite-difference grid. *Wave Motion*, 31(1):77–92.

Saenger, E. H., Krüger, O. S., and Shapiro, S. (2002). Simulation of effective elastic properties of 3D fractured medium. *72th Ann. Internat. Mtg., Soc. Expl. Geophys., Expanded Abstracts*, pages 1825–1828.

Saenger, E. H. and Shapiro, S. A. (2002). Effective velocities in fractured media: A numerical study using the rotated staggered finite-difference grid. *Geophys. Prosp.*, 50(2):183–194.

Wang, Z. and Nur, A., editors (2000). *Seismic and Acoustic Velocities in Reservoir Rocks*, pages 8–23. Society of Exploration Geophysics.